

Microscopic models for nucleon inelastic scattering

Workshop ESNT, 6-8 February 2013

E. Bauge, J.-P. Delaroche, **M. Dupuis**, S. Péru, CEA, DAM, DIF, France.
T. Kawano, LANL, New Mexico, USA.
J. Raynal, CEA Saclay, France.

Introduction

- (p,xp) or (n,xn) spectra: direct reactions, pre-equilibrium, evaporation (CN and fission fragments).

- **Pre-equilibrium models :**

- Quantum mechanical: FKK, TUL, NWY.
- Semi-classical: Exciton, intra-nuclear cascade.
- Hybrid ...

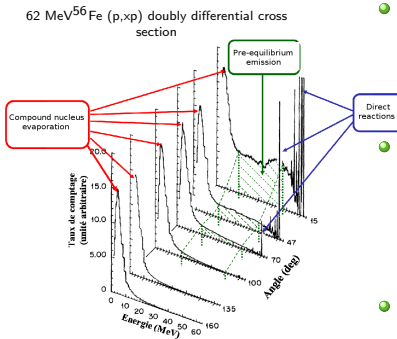
→ You can always fit the data with the right parameters set.

- FKK model:

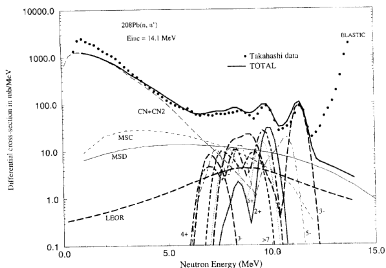
- MSC, MSD (one-step, two-steps ...): relative contributions not well known.
- Phenomenological ingredients: effective interaction, optical potential, level densities.
- compensating errors, need to fit parameters on cross-sections: not predictive.

- Different models give different answers for:

- Pre-equilibrium cross-section: changes probability of CN formation.
- Spin distribution of the residual nucleus with excitation energy (important for (n,n'γ)).



Pre-equilibrium and excitation of discrete states



P. Demetriou et al., Nucl. Phys. A 596, 67 (1996)

- High energy part of spectra: discrete + collective + pre-equilibrium cross-sections: each of these components is not well defined.
- Discrete excitations, collective states in the continuum:
 - Rely on inelastic scattering to discrete states measurements.
 - Response functions in the continuum (Giant resonances): from (e,e') , (h,h') , $(h,h'f)$.
 - depending on the nucleus, experimental information can be sparse: **collective response for $L > 3$, collective response for deformed targets.**

Need to perform pre-equilibrium calculations with:

- No adjustable parameters.
- The less phenomenological ingredients as possible.
- An accurate description of the nucleus excitations from a nuclear structure model that
 - Describes the measured spectroscopic properties well.
 - Predicts spectroscopic information for which experimental data are missing

→ **Microscopic models for direct pre-equilibrium emission.**

- 1 Microscopic models for nucleon elastic and inelastic scatterings
- 2 Diffusion élastique
- 3 Elastic scattering and inelastic scattering to discrete states
- 4 Direct pre-equilibrium emission for spherical targets: ^{90}Zr and ^{208}Pb
- 5 Direct pre-equilibrium emission for axially deformed nuclei: ^{238}U
- 6 Conclusions

Microscopic model for (shape) elastic and direct inelastic scattering

- Coupled equations for the elastic and some inelastic channels:

$$(E_{k_i} - T_0 - U_{00}) |u_0\rangle = \sum_{n=1}^k U_{0n} |u_n\rangle$$

$$(E_{k_f} - T_0 - U_{nn}) |u_n\rangle = \sum_{n' \neq n} U_{nn'} |u_{n'}\rangle, \dots$$

- Main ingredients \rightarrow one-body potentials $U_{nn'} = \langle \psi'_n | V_{eff} | \psi_n \rangle$, derived from:
 - target wave functions $\{\psi_n\}$: nuclear structure model
 - effective two-body interaction V_{eff} (g-matrix, JLM),
- Microscopic potentials:

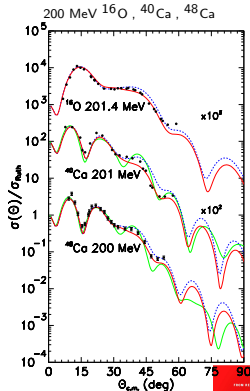
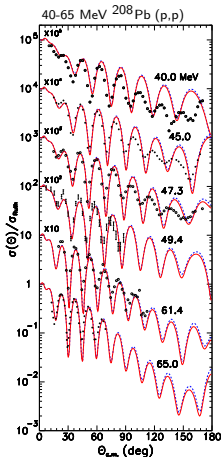
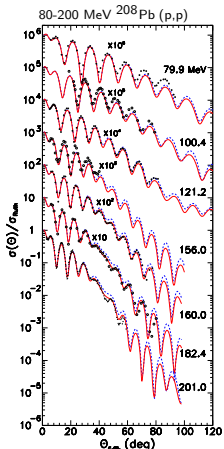
$$\langle N' | V_{eff} | N \rangle = \sum_{\alpha \alpha' k k'} \langle \alpha', k' | V_{eff} | \widetilde{\alpha}, k \rangle \rho_{\alpha \alpha'}^{N \rightarrow N'} a_{k'}^\dagger a_k$$

- Nuclear structure ingredients \rightarrow one-body density matrix:

$$\rho_{\alpha \alpha'}^{N \rightarrow N'} = \langle N' | a_{\alpha'}^\dagger a_\alpha | N \rangle$$

Nucleon elastic scattering

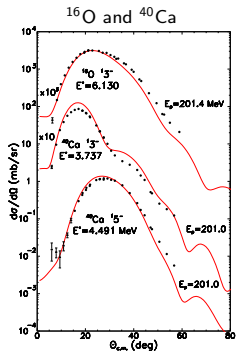
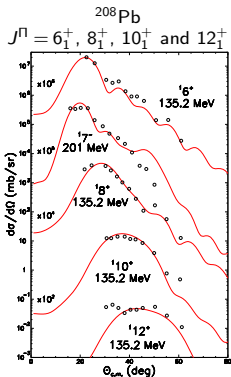
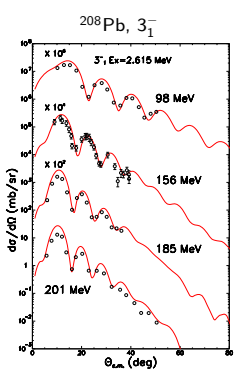
- Incident energy > 50 MeV \rightarrow **g-matrix** approximation: $V_{eff} = g(\rho, E)$
K. Amos, P.J. Dortmans, H.V. von Geramb, S. Karataglidis and J. Raynal, Adv. Nucl. Phys. 25 (2000) 275
- Fully microscopic OMP: $U_{00} = \langle \vec{0} | g(\rho, E) | \vec{0} \rangle$, $|\vec{0}\rangle \rightarrow$ RPA/D1S.
- **RPA/D1S+Melbourne g-matrix**: accurate predictions for $E > 50$ MeV: **No adjusted parameters**
- Comparison to **phenomenological models (JLM semi-microscopic)**.



Inelastic proton scattering to discrete states

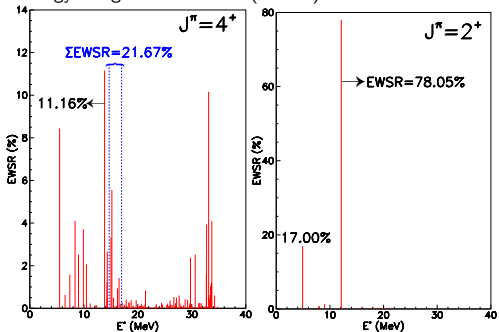
Distorted Waves Born Approximation (DWBA) $T_{f \leftarrow i} \simeq \langle \chi_f^{(+)}(\mathbf{k}_f) | U_{0N} | \chi_i^{(-)}(\mathbf{k}_i) \rangle$

- Ingredients : $V_{eff} \rightarrow$ Matrice g-Melbourne, $|\tilde{0}\rangle$, $|N\rangle$ Ground and excited states : RPA.
- Distorted waves : $T + U_{00}^{(+)} | \chi_i^{(+/-)}(\mathbf{k}_{i/f}) \rangle = E_{i/f} | \chi_i^{(+/-)}(\mathbf{k}_{i/f}) \rangle$
- Potentials : $U_{00} = \langle \tilde{0} | V_{eff} | \tilde{0} \rangle$ $U_{0N} = \langle N | V_{eff} | \tilde{0} \rangle$

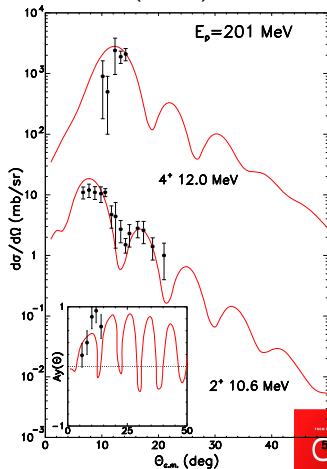


Inelastic scattering to discrete states: Giant Resonances

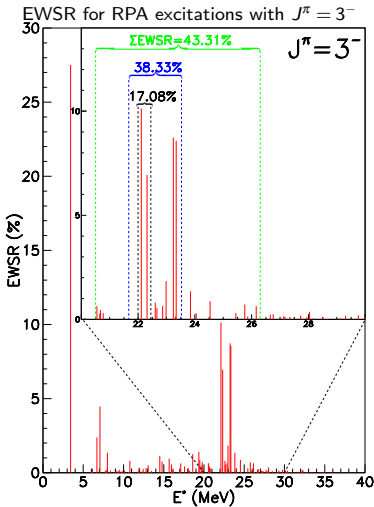
Energy Weighted Sum Rule (EWSR) for RPA excitations



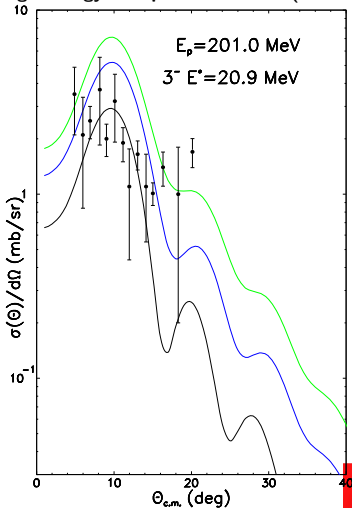
201 MeV ^{208}Pb (p, p'):
 Giant Hexadecapole Resonance (ISGHR),
 Giant Quadrupole Resonance (ISGQR)



Inelastic scattering to discrete states: Giant Resonances

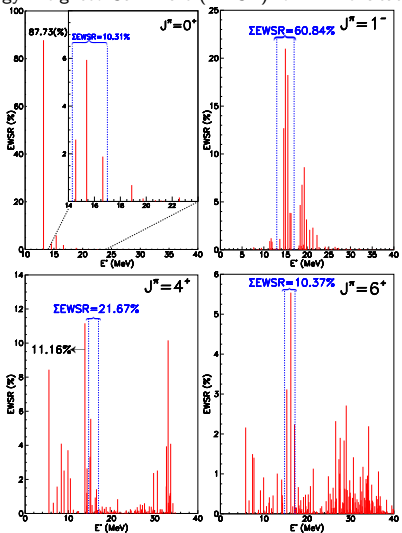


201 MeV ^{208}Pb (p,p'):
High Energy Octupole Resonance (HEOR)

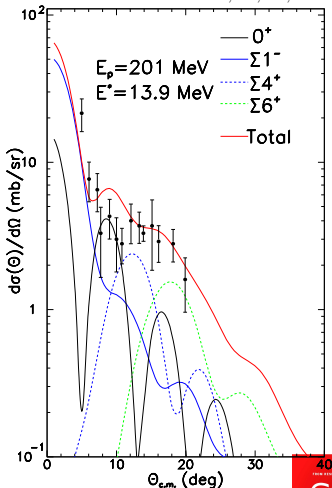


Inelastic scattering to discrete states: Giant Resonances

Energy Weighted Sum Rule (EWSR) for RPA excitations:



201 MeV ^{208}Pb (p,p'):
excitations with $J^\pi = 0^+, 1^-, 4^+, 6^+$



One-step direct process for spherical targets

Double differential cross section $(n,n')/(p,p')$ for the first order of direct pre-equilibrium emission (One Step Direct = OSD)

$$\frac{d\sigma(\mathbf{k}_i, \mathbf{k}_f)}{dE d\Omega_f} \sim \int dE \sum_N f(E_{k_i} - E_k - E_N) \left| \langle \chi_f^{(+)}(\mathbf{k}), N | V_{eff} | \chi_i^{(-)}(\mathbf{k}_i), \tilde{0} \rangle \right|^2$$

Ingredients

- Target states:

- RPA nuclear structure model with D1S Gogny interaction:

$|N\rangle = \sum_{ph} \left(X_{ph}^N a_p^\dagger a_h - Y_{ph}^N a_h^\dagger a_p \right) |\tilde{0}\rangle$ Account for Yrast, collective states (low energy and giant resonances) properties very well for closed-shell nuclei (see literature).

- Phonons :one particle-hole or hole-particle over the GS (doorway states).

- Comparison with particle-hole (p-h) excitations: $|N\rangle = a_p^\dagger a_h |HF\rangle$

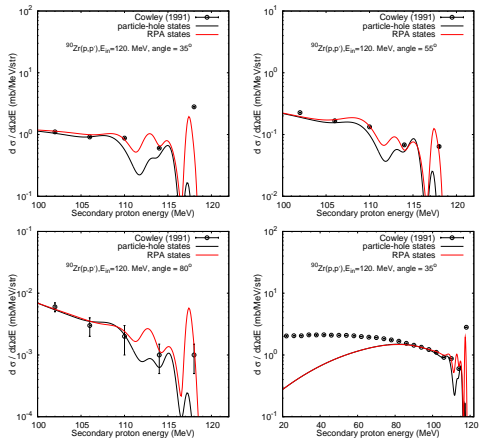
- Microscopic or phenomenological optical potential

- Effective interaction: g-matrix (produces non-local one-body potentials).

- $f(E_{k_i} - E_k - E_N) = \frac{1}{\pi} \frac{\Gamma_N}{(E_{k_i} - E_k - E_N + \Delta_N)^2 + \frac{\Gamma_N^2}{4}}$, $\Gamma_N = \Gamma^\downarrow + \Gamma^\uparrow$.

Émission directe de pré-équilibre pour la réaction : 120 MeV $^{90}\text{Zr}(p,p')^{90}\text{Zr}^*$

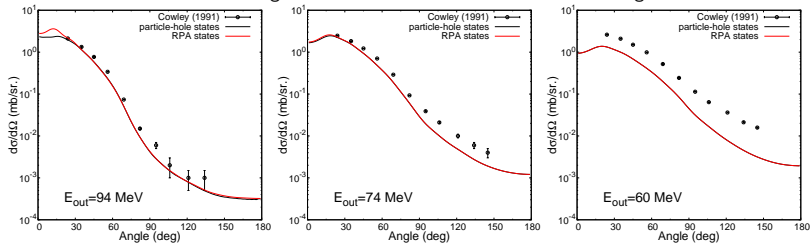
Spectres d'émission de neutrons à différents angles d'émission :



- Émission à haute énergie : bien décrite à tous les angles ($E_{in} - E_{out} < 25$ MeV).
 - Processus one-step direct: décrit l'émission aux angles avant jusqu'à $E_{in} - E_{out} \simeq 50$ MeV.
 - RPA/p-h: révèle l'influence de la **collectivité** jusqu'à $E_{in} - E_{out} = 15$ MeV.
 - Émission à plus haute énergie et angles arrières : implique d'autres mécanismes de réaction (Multi-step direct, Multi-Step Compound, évaporation).
- Pas de paramètres ajustés**

Émission directe de pré-équilibre pour la réaction : 120 MeV $^{90}\text{Zr}(p,p')^{90}\text{Zr}^*$

Distributions angulaires des neutrons émis à différentes énergies :



- Émission aux angles avant bien décrite jusqu'à $E_{in} - E_{out} \simeq 50$ MeV.
- Émission à plus haute énergie et angles arrières : implique d'autres mécanismes de réaction (Multi-step direct, Multi-Step Compound, évaporation).

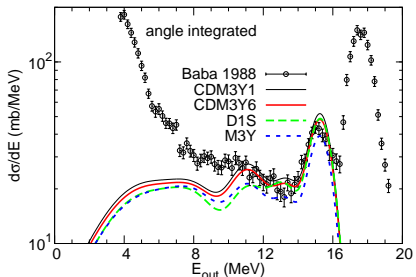
Pas de paramètres ajustés

Ingrédients "phénoménologiques" du modèles:

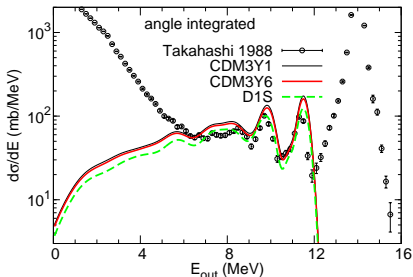
- Interaction effective Gogny D1S pour les calculs de structure, interaction nue de Bonn-B pour définir la matrice-g.
- Largeurs (Damping+escaped).

Section efficace one-step direct : influence de l'interaction effective

18 MeV $^{90}\text{Zr}(n,n')$

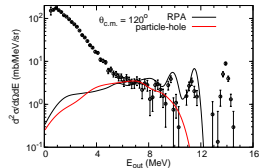
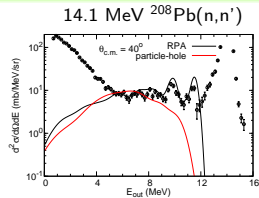
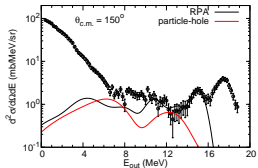
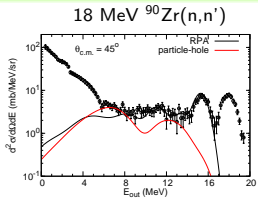


14.1 MeV $^{208}\text{Pb}(n,n')$



- Émission à haute énergie globalement bien reproduites : **pas de paramètres ajustés**.
- Différentes interactions : variation des sections efficaces de l'ordre de 20%.

One-step direct emission process: impact of collective states



- OSD cross section with p-h excitations:

→ Underestimate the neutron emission at high energy. In phenomenological analyzes, inelastic components for discrete states are added to the OSD pre-equilibrium cross section.

- OSD cross section with RPA excitations:

→ account for the neutron emission measured at high energy (above evaporation component).

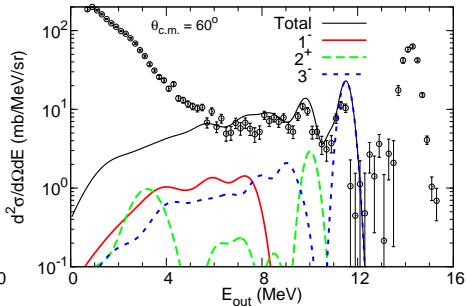
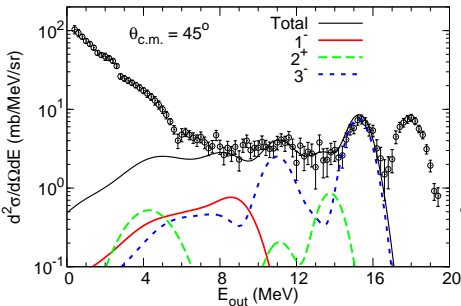
→ coherent description of collective (vibrations) and non-collective (close to p-h) excitations: low energy collective states, giant resonances, non-natural parity, etc.

→ G-matrix at low incident energy (10-20 MeV) : overall uncertainty of ~ 20 % on OSD cross sections.

Décomposition en spin et parité

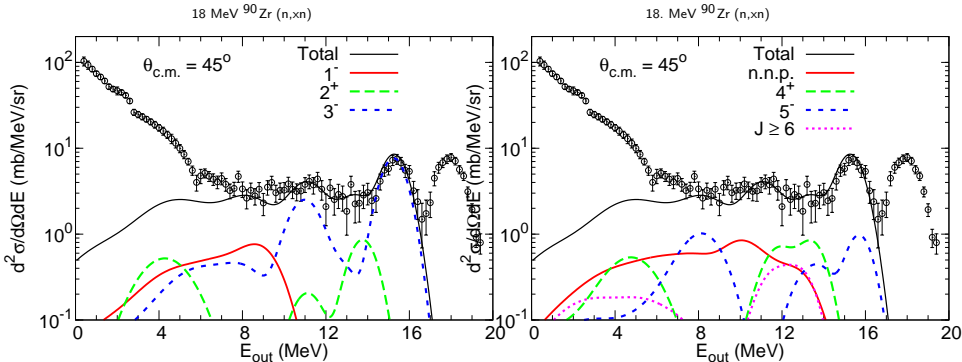
18 MeV ^{90}Zr (n,xn)

14.1 MeV ^{208}Pb (n,xn)



- Forte contribution de la LEOR ($E_{out}=11$ MeV à droite, 9 MeV à gauche).
- Effet des résonances géantes réduit à ces énergies incidentes : ISGQR ($E_{out}=3-4$ MeV).

Spin-parity components of the OSD cross section



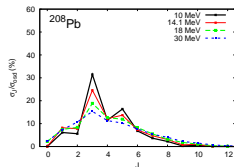
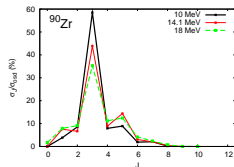
● Strong contribution of collective states from $J^\pi = 2 - 5$.

→ An accurate description of the collective content of the target states is necessary.

M. Dupuis, T. Kawano, J.-P. Delaroche, E. Bauge, **PRC83, 014602 (2011)**.

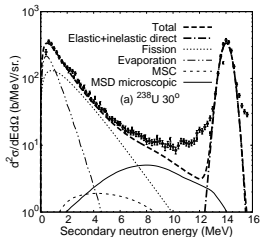
	E_{in} (MeV)	σ_{osd}/σ_R (%)	% $\pi = (-)^J$	% $\pi = (-)^{J+1}$
^{90}Zr	10	10.5	91.8	8.2
	14.1	15.9	86.7	13.3
	18	20.7	85.0	15
^{208}Pb	10	21.9	84.5	15.5
	14.1	26.7	83.2	16.8
	18	32.9	81.2	18.8
	30	31.8	79	21

RPA natural parity states

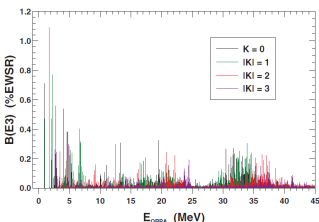
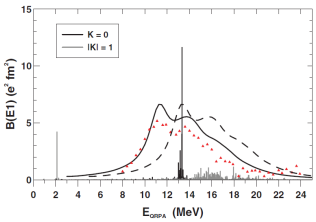


Direct pre-equilibrium emission for axially deformed targets

- Motivations: calculations with p-h excitations
 ⇒ **underestimates neutron emission at high energy.**
- Long-standing issue: ENDF (and others) use pseudo-states, with properties tuned to reproduce the high energy neutron emission



Recently: self-consistent deformed QRPA calculations with the D1S Gogny interaction for ^{238}U .
 S.Peru, G.Gosselin, M.Martini, M.Dupuis, S.Hilaire, J.-C.Devaux, *Phys.Rev.C* **83**, 014314 (2011).
 Prediction of collective excitations



Direct emission for axially deformed targets

- Rotational bands → collective excitations at very low energy: coupled channels method.

$$\frac{\hbar^2}{2m_i} \left(\frac{d^2}{dr^2} - \frac{l_i(l_i+1)}{r^2} + k_i^2 \right) f_i(r) = \sum_{i'} \langle i'IM | \hat{V} | iIM \rangle f_{i'}(r), i \equiv (l_i, j_i), \alpha_i J_i$$

- Model with local coupling potentials built from the microscopic description of the target states: JLM convolution model (convolution V_{eff} with local matter densities).
- Effective interaction V_{eff} : JLM potential JLM, based on a calculation in nuclear matter, renormalized to reproduced nucleon elastic scattering data (and charge exchange) from 1 keV to 200 MeV (spherical and deformed targets).
E. Bauge, J. P. Delaroche, and M. Girod, Phys. Rev. C63, 024607 (2001), Phys. Rev. C58, 1118 (1998).

Excited states of the axially deformed target

- QRPA method: provides excitation in the intrinsic frame. Axial deformation: good quantum numbers are the projection K of the total angular momentum other the symmetry axis Oz and the parity Π

$$|\alpha K \Pi\rangle = \Theta_{\alpha K \Pi}^+ |\tilde{0}_I\rangle = \frac{1}{2} \sum_{ij \in (K \Pi)} \left(X_{ij}^{\alpha K \Pi} \eta_{ip_i \Omega_i}^+ \eta_{jp_j \Omega_j}^+ - (-)^K Y_{ij}^{\alpha K \Pi} \eta_{ip_i - \Omega_i} \eta_{jp_j - \Omega_j} \right) |\tilde{0}_I\rangle$$

- Two quasi-particles excitations (similar to p-h excitations for nuclei without pairing correlations):

$$|\alpha K \Pi\rangle = \eta_i^+ \eta_j^+ |HFB\rangle$$

- Nuclear states in the laboratory frame: projection over the total angular momentum \rightarrow rotational band, with angular momenta $J \geq K$

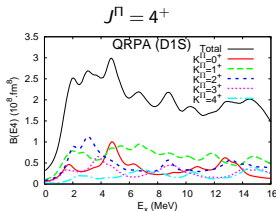
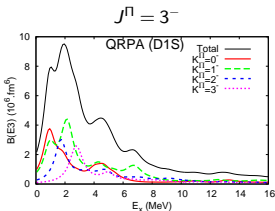
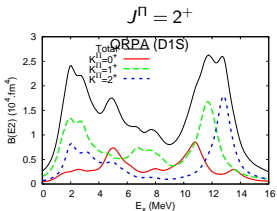
$$|\alpha J M K \Pi\rangle = \sqrt{\frac{2J+1}{16\pi^2}} \int d\Omega \mathcal{D}_{MK}^J(\Omega) R(\Omega) |\alpha K \Pi\rangle + (-)^{J+K} \mathcal{D}_{M-K}^J(\Omega) R(\Omega) |\alpha \bar{K} \Pi\rangle$$

$$E_{\alpha K J \Pi} = E_{\alpha K \Pi} + \frac{J(J+1) - K^2}{2\mathcal{I}^2}$$

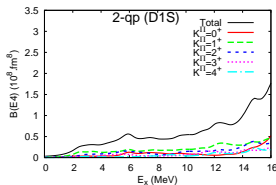
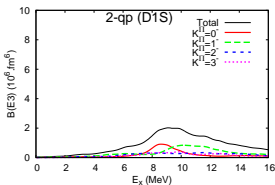
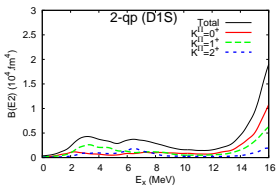
QRPA and 2-qp response functions in ^{238}U

Reduced transition probabilities (proton+neutron) $B(EJ) \sim \int \rho_{J,\alpha K \Pi}^{\delta}(r) r^{J+2} dr$ ($L > 2$) :

QRPA



2 quasi-particles



- strength moved at low excitation energy for all multiplicities.
- Self-consistent QRPA calculations with the D1S Gogny interaction: performed in a large configuration space (12 harmonic oscillators major shell: up to 25,000 2qp configurations for each projection K). *S.Peru, G.Gosselin, M.Martini, M.Dupuis, S.Hilaire, J.-C.Devaux, Phys.Rev.C 83, 014314 (2011).*

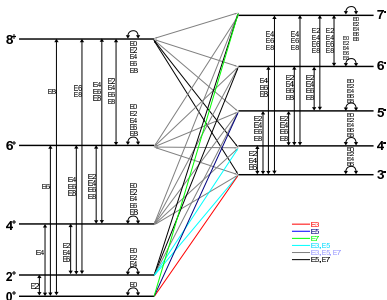
Direct pre-equilibrium emission for axially deformed nuclei

Doubly differential cross section:

$$\frac{d\sigma(\mathbf{k}_i, \mathbf{k}_f)}{dE d\Omega_f} \sim \int dE \sum_N f(E_{k_i} - E_k - E_N) \frac{d\sigma_N(\mathbf{k}_i, \mathbf{k})}{d\Omega}$$

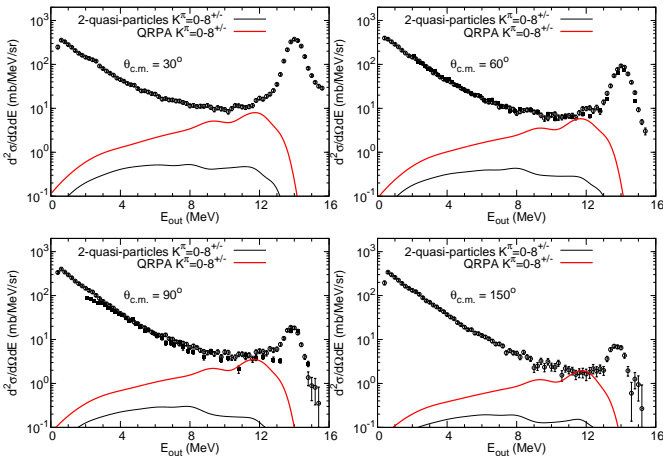
Sum over target states: $\sum_N = \sum_{K^\pi} \sum_{J \geq K}$

→ Intrinsic excitations (band heads), each state of a rotational band
Coupling scheme used independently for each intrinsic excitation:



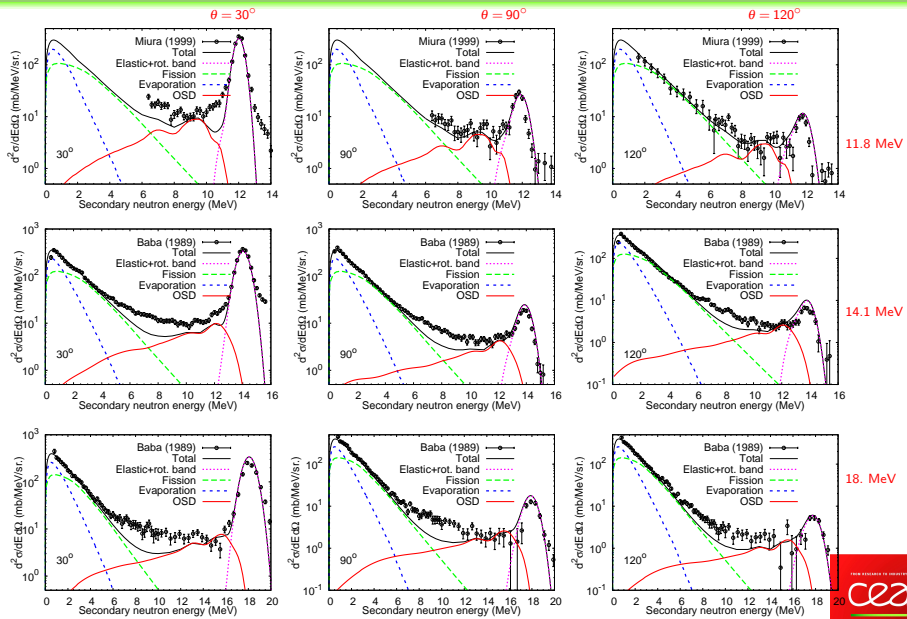
→ performed for $K^\pi \leq 8^{+/-}$, and $J \geq K \leq 8$ ($\sim 2000-8000$ intrinsic excitations for $E = 11 - 18$ MeV).

Direct pre-equilibrium emission: 14.1 MeV (n,n') ²³⁸U



- Comparison QRPA / 2 quasi-particles : collective transitions very important.
- Strength of 2qp excitations concentrated above 10 MeV.
- Larger discrepancies at forward angles at 14.1 MeV.

Direct pre-equilibrium emission for: 11-18 MeV (n,n') ²³⁸U

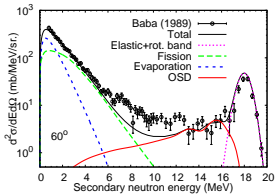
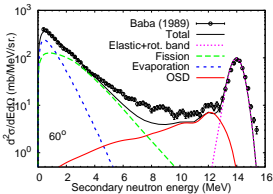
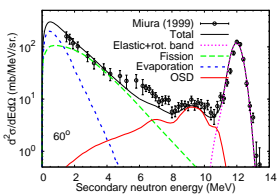


11.8 MeV

14.1 MeV

18. MeV

Direct pre-equilibrium emission for: 11-18 MeV (n,n') ²³⁸U



Improve the present direct pre-equilibrium emission model for axially deformed targets

- Non-natural parity transitions: tensor interactions.
- Model approximations (local density approximation, coupling scheme), ingredients are of course not perfect (effective interaction, damping widths, QRPA response functions): need to estimate error on overall normalization.

Microscopic model with realistic ingredients and no adjustable parameter: discrepancies with data allow to identify model deficiencies, important reaction mechanisms that were neglected.

- High one-phonon state density: excitation of two-phonons states → multi-step could be important even at these low incident energies.
- Multi-step compound contributions ?
- Evaporation of fission fragments well described ?
- Blame the data ? Extend these calculation to other targets (²³²Th).

Conclusions

Direct pre-equilibrium emission for spherical the targets ^{90}Zr ^{208}Pb .

- Microscopic model using RPA states: one-step direct (n,n') component under 20 MeV
- Good description of emission at high energy, no adjustable parameters.
- No arbitrary distinction between direct reactions and pre-equilibrium process.

Direct emission: a precise description of the target spectrum collectivity content is necessary.

Direct pre-equilibrium emission for the axially deformed target ^{238}U

- Microscopic model using QRPA states including: one phonon excitations (n,n') component under 20 MeV.
- Large contributions from collective states (as seen (n,n') studies with ^{90}Zr and ^{208}Pb).
- Account for the major part of the high energy emission.
- Microscopic model with realistic ingredients and no adjustable parameter: can be used to identify important neglected mechanisms (two-steps below 20 MeV ?), provides constraint to models that are used to calculate other reaction mechanisms (MSC, evaporation).

THANK YOU

FOR YOUR ATTENTION